

Original Article

Correlations Between Trabecular Bone Score, Measured Using Anteroposterior Dual-Energy X-Ray Absorptiometry Acquisition, and 3-Dimensional Parameters of Bone Microarchitecture: An Experimental Study on Human Cadaver Vertebrae

Didier Hans,¹ Nicole Barthe,^{2,3} Stephanie Boutroy,⁴ Laurent Pothuaud,^{5,†}
 Renaud Winzenrieth^{*,5} and Marc-Antoine Krieg¹

¹Department of Bone and Joint Diseases, Center of Bone Diseases, Lausanne University Hospital, Lausanne, Switzerland; ²Biophysics Laboratory, University Victor Segalen, Bordeaux, France; ³Department of Radiology, University Hospital, Bordeaux, France; ⁴INSERM U831, Lyon University Hospital, Lyon, France; and ⁵Med-Imaps, Biomedical technology center, Xavier Arnoz Hospital, Bordeaux University Hospital, Pessac, France

Abstract

Developing a novel technique for the efficient, noninvasive clinical evaluation of bone microarchitecture remains both crucial and challenging. The trabecular bone score (TBS) is a new gray-level texture measurement that is applicable to dual-energy X-ray absorptiometry (DXA) images. Significant correlations between TBS and standard 3-dimensional (3D) parameters of bone microarchitecture have been obtained using a numerical simulation approach. The main objective of this study was to empirically evaluate such correlations in anteroposterior spine DXA images. Thirty dried human cadaver vertebrae were evaluated. Micro-computed tomography acquisitions of the bone pieces were obtained at an isotropic resolution of 93 μm . Standard parameters of bone microarchitecture were evaluated in a defined region within the vertebral body, excluding cortical bone. The bone pieces were measured on a Prodigy DXA system (GE Medical-Lunar, Madison, WI), using a custom-made positioning device and experimental setup. Significant correlations were detected between TBS and 3D parameters of bone microarchitecture, mostly independent of any correlation between TBS and bone mineral density (BMD). The greatest correlation was between TBS and connectivity density, with TBS explaining roughly 67.2% of the variance. Based on multivariate linear regression modeling, we have established a model to allow for the interpretation of the relationship between TBS and 3D bone microarchitecture parameters. This model indicates that TBS adds greater value and power of differentiation between samples with similar BMDs but different bone microarchitectures. It has been shown that it is possible to estimate bone microarchitecture status derived from DXA imaging using TBS.

Key Words: Bone microarchitecture; DXA (dual-energy X-ray absorptiometry); human cadaver vertebrae; TBS (trabecular bone score).

Introduction

Osteoporosis is a skeletal disorder characterized by compromised bone strength, which predisposes an affected

individual to bone fractures (*1*). The management of osteoporosis requires accurate clinical assessments of bone strength and fracture risk. Dual-energy X-ray absorptiometry (DXA) is commonly used to diagnose osteoporosis in clinical practice, providing accurate estimates of bone mass through the evaluation of bone mineral density (BMD). However, BMD is not always an accurate predictor of fracture risk (*2–5*). One reason may be that bone mass is not the only contributor to bone strength. Consequently, evaluating some other bone parameter, such as bone microarchitecture, could significantly

Received 09/07/10; Revised 05/16/11; Accepted 05/17/11.

[†]Deceased on August 14, 2009.

*Address correspondence to: Renaud Winzenrieth, PhD, Med-Imaps, Biomedical technology center, Xavier Arnoz Hospital, Bordeaux University Hospital, Pessac, France. E-mail: renaudwinzenrieth@yahoo.fr

enhance the assessment of bone strength (6–8) and fracture risk.

In recent years, a number of developments have contributed to bone microarchitecture assessment techniques. Among the noninvasive techniques, (peripheral) quantitative computed tomography (9) and magnetic resonance imaging (10) allow for the direct or indirect measurement of bone microarchitecture, and both have benefited from significant enhancements in acquisition technology and/or image analysis. Nonetheless, these two techniques remain impractical for the routine screening and clinical management of osteoporosis because of high costs, patient inconvenience, and their availability for such diseases. Histomorphometric assessment of iliac crest bone biopsies remains the gold-standard method for the direct assessment of bone microarchitecture, but this technique is invasive and not directly 3 dimensional (3D). A major challenge, therefore, has been to develop some novel technique that allows for the efficient, noninvasive clinical evaluation of bone microarchitecture status. 2D X-ray-based images, such as plain radiographs, have been investigated widely as a more practical alternative for the noninvasive and indirect assessment of bone microarchitecture. Different gray-level features have been explored, including fractal dimension and Fourier analysis, among others (11–16).

Over the past several years, DXA technology has advanced dramatically, in terms of both its hardware and software components (17). Recent generations of DXA systems provide not only accurate and reproducible measurements of BMD but also the opportunity to use high-quality DXA scans in place of standard X-rays to confirm and characterize existing vertebral fractures. Hence, Genant et al's (18) indices of vertebral fracture (19) and certain indices related to hip geometry (20,21) can be evaluated directly from high-quality DXA images. More recently, a new application called *hip structure/hip strength analysis* allows us to obtain information related to bone strength of the proximal femur (22,23). These macroscopic geometrical measurements constitute risk factors that are independent of BMD, and the ability to obtain them from the same DXA examination is an additional advantage. Langton et al (24) have developed a new technique, called *finite element analysis of X-ray images (FEXI)*, which uses a finite element analysis model applied to DXA gray-level images. This technique permits the evaluation of a new DXA-based measure: "*FEXI stiffness*." Boehm et al (25) introduced an algorithm to evaluate the hip DXA scans using quantitative image analysis procedures based on *Minkowski Functionals*. This new DXA-based measure considers bone mineral distribution in the proximal femur, instead of just BMD, and may be well suited to enhance standard densitometric evaluations as a predictor of hip fracture risk.

Trabecular bone score (TBS) is a new gray-level texture measurement that can be applied to DXA images (24). TBS is based on the measurement of the experimental variogram derived from a gray-level DXA image. In previous studies, we identified significant correlations between TBS—as evaluated from simulated 2D-projection micro-computed tomography (μ -CT) images—and standard 3D parameters of bone

microarchitecture—evaluated using high-resolution μ -CT reconstructions—in sets of human vertebral bone pieces (26). At 93- μ m plane resolution, strong significant correlations have been obtained between TBS and Parfitt's microarchitecture parameters, such as connectivity density (connD: $0.856 \leq r \leq 0.862$, $p < 0.001$); trabecular number (TbN: $0.805 \leq r \leq 0.810$, $p < 0.001$); and trabecular spacing (TbSp: $-0.714 \leq r \leq -0.726$, $p < 0.001$), regardless of the X-ray energy used for the projection (26). On the other hand, the effects of image resolution degradation (from 93- to 1488- μ m plane resolution) and noise have been studied (27) using μ -CT images. Significant correlations were obtained between TBS and 3D microarchitecture parameters, regardless of image resolution, up to a certain level. Strong correlations were obtained with connD ($0.843 \leq r \leq 0.867$), TbN ($0.764 \leq r \leq 0.805$), and TbSp ($-0.701 \leq r \leq -0.638$), and with those up to a resolution of 744 μ m. From a clinical point of view, several cross-sectional studies have shown the ability of TBS to discriminate subjects with vertebral fractures from healthy subjects matched for age, BMD, or both (28–30). It has also been demonstrated that TBS is relevant in secondary osteoporosis (31–33). Finally, it has been shown that spine TBS predicts major osteoporotic fractures as well as, and independent of, spine BMD, and that combining the TBS microarchitecture index with BMD from conventional DXA incrementally improves fracture predictions in postmenopausal women (34,35).

The main objective of the present study was to determine whether the 2D/3D correlations previously identified during the feasibility study could be reproduced when TBS of anteroposterior (AP) DXA images are considered.

Materials and Methods

Human Cadaver Vertebrae

Thirty human cadaver lumbar vertebrae were obtained from the Anatomy Laboratory at the University Hospital of Bordeaux (France). These dried bone pieces were free of bone marrow, in accordance with standard procedures. Whole vertebrae (an intact segment of the spine including the superimposing posterior elements) were considered in this study. In addition, these vertebrae were protected using a thin layer of epoxy resin. It has been verified that this thin layer has no effect on CT or DXA acquisitions.

3-Dimensional Measurements Assessed by Micro-Computed Tomography

3D reconstruction of bone pieces (Fig. 1A) was done using high-resolution CT (μ -CT) (eXplore Locus; GE Medical Systems, London, Ontario, Canada). The in-slice voxel size of the 3D volume acquisition is $93 \times 93 \times 93 \mu\text{m}$. Each gray-level μ -CT reconstruction image was binarized by means of global thresholding, with the threshold value automatically determined by gray-level histogram analysis (MicroView 2.1.2—Bone Analysis/Auto Threshold plugin; GE Healthcare, Madison, WI). A specific region of measurement (trabecular

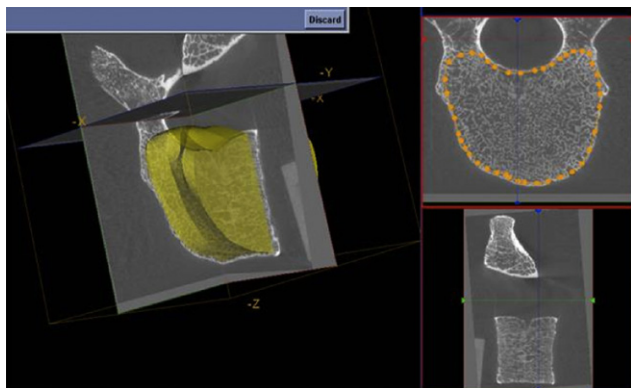


Fig. 1. MicroView software platform allowing for (1) definition of the 3-dimensional (3D) volume of analysis (inside the vertebral body, excluding the cortical slice) using the “ROI (Region Of Interest)-spline” plugin and (2) calculation of “standard” 3D parameters of bone microarchitecture using the “Advanced Bone Analysis” plugin.

compartment—Fig. 1B), excluding cortical bone, was defined inside the vertebral body. Standard parameters were calculated inside this region, using the parallel-plate model (36), following the recommended nomenclature (37), and using specific software: Advanced Bone Analysis plugin (Fig. 1B) in MicroView software (MicroView 2.1.2). The measured parameters were as follows: bone volume/total volume (BV/TV, expressed as a ratio without units or in %); trabecular thickness (TbTh, expressed in mm); TbSp (expressed in mm); TbN (expressed in mm^{-1}); and connD (expressed in mm^{-3}).

Trabecular Bone Score Measurement Assessed by Dual-Energy X-Ray Absorptiometry

TBS is an index that characterizes the bone microstructure obtained by macroscopic representation (DXA image). A synthetic description of the TBS concept is proposed in Appendix 1. TBS is directly derived from the raw data of the device sensor (i.e., the raw image differs from the displayed image).

The bone pieces were measured 3 times consecutively (the average of the 3 measurements was used for all statistics to take into account DXA acquisition variability) on a Prodigy DXA system (GE Medical-Lunar, Madison, WI) with a customized experimental system (Fig. 2) that included (1) a positioning system to allow for AP acquisition and (2) a stack of plates of high-density polyethylene + polyvinyl chloride (PVC) mimicking soft tissue (equivalent thickness = 17 cm, 26% fat). After acquisition, the DXA scan was analyzed using the manufacturer’s software (enCORE 2004; GE Medical-Lunar) and the bone map manually positioned as the inner rectangle of the vertebral body. BMD (expressed in g/cm^2) was evaluated directly using enCORE 2004 software. Then the DXA files were exported to a specific workstation for TBS calculation. In addition, to compare vertebral microarchitecture assessed by TBS and high-resolution CT, normalization of TBS values by the projected vertebral surface was performed.

Statistical Analysis

Statistical analysis was performed using MedCalc software (v9.0.1.1; MedCalc Software, Mariakerke, Belgium) to generate descriptive statistics for each investigated parameter (mean, standard deviation [SD]: minimum and maximum values); to calculate Pearson’s correlation coefficients (r and p values); and to perform multiple (linear) regression analysis.

The root mean square (RMS) and percent methods were used to calculate the TBS SD of the precision error (RMS SD) and the TBS SD corrected for the mean of paired-measurements precision error coefficient of variation in % (CV%), respectively, considering the whole vertebral set, in accordance with ISCD recommendations. The 95% confidence interval for least significant change (LSC) was defined for the CV% precision error by multiplying by 2.772 (38).

For each investigated parameter, a box-and-whisker plot was generated to ensure against extreme outliers, defined as any value that is smaller than the lower quartile minus 3 times the interquartile range, or larger than the upper quartile plus 3 times the interquartile range. In addition, the cumulative frequency distribution was plotted, allowing for a visual

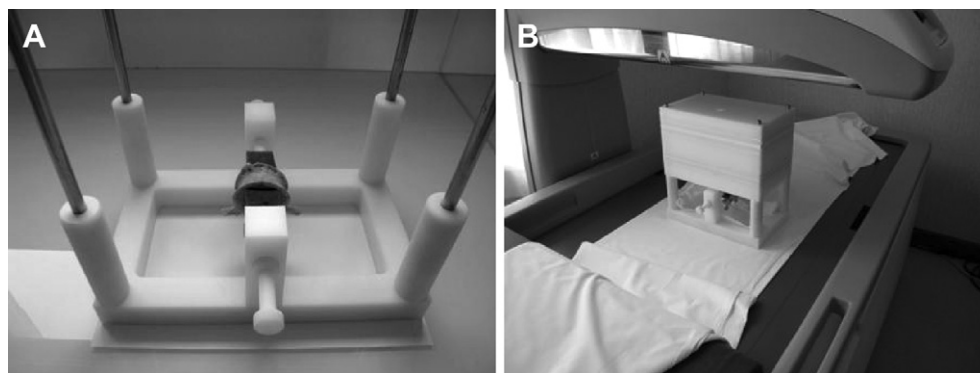


Fig. 2. Positioning system dedicated to dual-energy X-ray absorptiometry experiments on human cadaver vertebrae, including (A) a positioning system allowing for anteroposterior acquisition and (B) a stack of plates of High density polyethylene + PolyVinyl Chloride mimicking soft tissue (equivalent thickness = 17 cm, 26% fat).

comparison of the observed frequency distribution against a theoretical normal distribution. An X-Y scatter plot was used to identify any correlations between parameters; the regression line of the correlation was determined, and the RMS error between observed and estimated values was calculated.

Multiple regression analysis was performed using backward variable selection. Potential significant cofactors were taken into account. Where appropriate, analyses were 2 tailed, and $p = 0.05$ was set as the threshold both for statistical significance and for inclusion in the final regression model.

Results

Descriptive Statistics

The values of TBS varied from 1.055 to 1.511 (Table 1), and the analysis of TBS value distribution failed to identify any outliers. BMD values ranged from 0.817 to 1.568 g/cm² (Table 1), again without any evidence of outliers. Hence, the data set of the study, derived from 30 human cadaver vertebrae, appeared to be representative of routine clinical values for TBS and BMD. Analysis of the distribution for the various 3D bone microarchitecture parameters again failed to reveal any outliers.

Trabecular Bone Score Reproducibility

Evaluation

From the whole set of vertebrae, the TBS RMS SD value was 0.02. Considering the relative precision error, TBS CV% was 1.63% for an LSC₀₅ of 4.51%.

Correlation With Bone Microarchitecture

Parameters

The following correlations were identified between TBS and 3D parameters of bone microarchitecture (Table 2 and Fig. 3A): $r = 0.52$ ($p = 0.0033$) between TBS and BV/TV; $r = -0.56$ ($p = 0.0014$) between TBS and TbTh; $r = -0.63$ ($p < 0.0001$) between TBS and TbSp; $r = 0.75$ ($p < 0.0001$) between TBS and TbN; and $r = 0.82$ ($p < 0.0001$)

between TBS and connD. The highest correlation was between TBS and connD, TBS explaining about 67.2% of the variance in 3D connectivity. The relationship between TBS and 3D bone microarchitecture parameters was such that low values of TBS were indicative of “weak microarchitecture, associated with low connectivity, high TbSp, and a reduced number of trabeculae”; conversely, high values of TBS indicated “strong microarchitecture, with high connectivity, low TbSp, and a greater number of trabeculae.”

A low degree of correlation was evident between TBS and BMD parameters (Fig. 3A), despite being obtained from the same site and Region Of Interest (ROI)-matched DXA evaluation. This correlation was characterized by the linear regression model: $TBS = 1.060 + 0.222 * BMD$ ($r = 0.27$). A high level of correlation was obtained between TBS and connD parameters (Fig. 3B), obtained from DXA and μ -CT acquisitions, respectively. This correlation was characterized by the linear regression model: $TBS = 0.888 + 0.088 * connD$ ($r = 0.82$). Higher correlations between BMD and 3D parameters of bone microarchitecture were obtained between BMD and BV/TV ($r = 0.73$; $p < 0.0001$) and between BMD and TbSp ($r = -0.63$; $p = 0.0002$). A statistically significant correlation was also evident between BMD and TbN ($r = 0.60$, $p = 0.0005$). No significant correlation was identified between BV/TV and TbTh ($r = 0.27$, $p = 0.153$).

The combination of TBS and BMD in a linear regression model increased the degree of variance explained for BV/TV ($r = 0.81$, vs 0.73 and 0.52 for TBS and BMD cofactors respectively); TbTh ($r = 0.70$, vs -0.56 and 0.27, respectively); TbSp ($r = -0.79$, vs -0.63 and -0.63 , respectively); TbN ($r = 0.85$, vs 0.75 and 0.60, respectively); and connD ($r = 0.90$ vs 0.82 and 0.58, respectively).

Model for Trabecular Bone Score Interpretation

Using multivariate linear regression analysis, an interpretation model, $TBS = F(BV/TV, TbTh)$, was established with an RMS error of 0.026 (see Appendix 2). This equation was obtained by substituting $connD = F(BV/TV, TbTh)$ into the

Table 1
Descriptive Statistics for Each Investigated Parameter

Parameter	Evaluation	Designation	Unit	Mean	SD	Minimum	Maximum
BV/TV	μ -CT acquisition ^a	Bone volume/trabecular volume	—	0.288	0.046	0.185	0.376
TbTh	μ -CT acquisition ^a	Trabecular thickness	mm	0.228	0.015	0.197	0.251
TbSp	μ -CT acquisition ^a	Trabecular spacing	mm	0.543	0.129	0.348	0.874
TbN	μ -CT acquisition ^a	Trabecular number	mm ⁻¹	1.457	0.239	0.933	1.793
connD	μ -CT acquisition ^a	Connectivity density	mm ⁻³	4.652	1.407	1.326	6.593
BMD	DXA acquisition ^b	Bone mineral density	g/cm ²	1.063	0.18	0.817	1.568
TBS	DXA acquisition ^b	Trabecular bone score	—	1.314	0.136	1.055	1.511

Abbr: BV/TV, bone volume/total volume; TbTh, trabecular thickness; TbSp, trabecular spacing; TbN, trabecular number; connD, connectivity density; TBS, trabecular bone score; BMD, bone mineral density; SD, standard deviation; μ -CT, micro-computed tomography; DXA, dual-energy X-ray absorptiometry.

^aEvaluation inside the vertebral body excluding cortical slice and posterior elements.

^bEvaluation from an anteroposterior DXA image.

Table 2
Correlations Between Dual-Energy X-Ray Absorptiometry–Based Parameters (TBS and BMD) and 3-Dimensional Parameters of Bone Microarchitecture

	BV/TV	TbTh	TbSp	TbN	ConnD
TBS					
Correlation coefficient (r)	0.528	−0.553	−0.643	0.751	0.821
Correlation significance (p)	0.0033	0.0015	<0.0001	<0.0001	<0.0001
BMD					
Correlation coefficient (r)	0.711	0.326	−0.587	0.550	0.531
Correlation significance (p)	<0.0001	0.0790	0.0007	0.0016	0.0026
TBS and BMD					
Correlation coefficient (r)	0.812	0.713	−0.793	0.853	0.901
TBS cofactor significance (p)	0.0018	0.0001	0.0001	<0.0001	<0.0001
BMD cofactor significance (p)	<0.0001	0.0025	0.0005	0.0004	0.0001

Abbr: BV/TV, bone volume/total volume; TbTh, trabecular thickness; TbSp, trabecular spacing; TbN, trabecular number; connD, connectivity density; TBS, trabecular bone score; BMD, bone mineral density.

equation $TBS = F(\text{connD})$. The graphical representation of this regression model consisted of plotting isocurves for identical TbTh in the (BV/TV, TBS) 2D plot. Hence, it was possible to interpret variations in TBS based on the analysis of simultaneous variations in BV/TV and TbTh (legends of Figs. 4 and 5).

Discussion

TBS was significantly correlated with the 3D parameters of bone microarchitecture, and this was mostly independent of any association with BMD. The highest degree of correlation was apparent between TBS and connD, with TBS explaining 67.2% of the variance in 3D connectivity. The relationship between TBS and 3D bone microarchitecture parameters was such that a low TBS was indicative of weak or degraded

microarchitecture, associated with low connectivity, high TbSp, and a reduced number of trabeculae, whereas a high TBS reflected strong microarchitecture, with high connectivity, low TbSp, and a greater number of trabeculae. In this study, the 95% confidence interval ($\pm 2 * SD$) overlapped 70–80% of the 95% confidence interval for the TBS values, as determined across the L1–L4 lumbar spine region in a routine clinic population of 5942 women older than 45 years (39). The 95% confidence interval ($\pm 2 * SD$) for BMD overlapped from 92% to 100% of the 95% confidence interval of BMD values evaluated across the L1–L4 lumbar spine region in the same routine clinic population. These results were obtained experimenting on human cadaver vertebrae using a Prodigy DXA system. However, similar results were obtained on Lunar iDXA (GE-Lunar, Madison, WI) and Discovery (Hologic Inc., Bedford, MA) densitometers (data not shown).

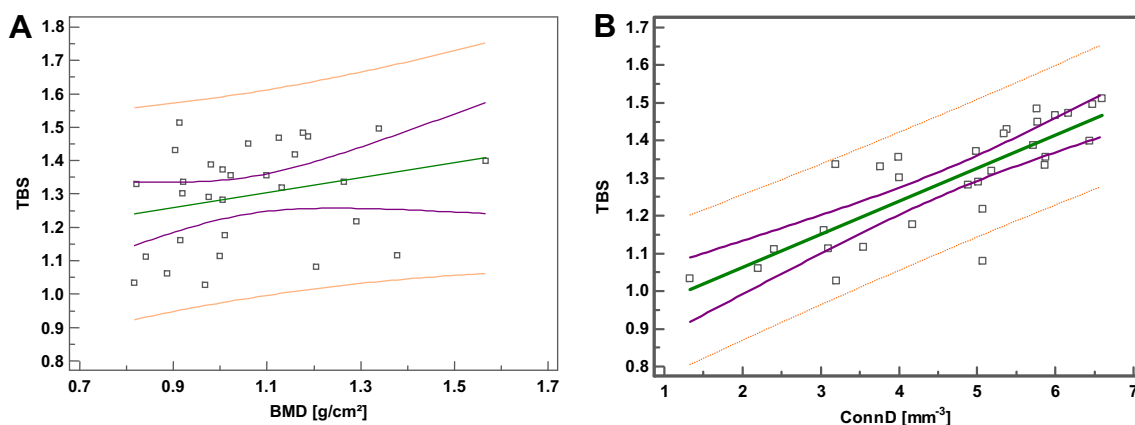


Fig. 3. (A) X-Y scatter plot visualizing the correlation between TBS and BMD, as evaluated using the same DXA acquisition. This low correlation is characterized by $r = 0.27$ ($p = 0.1569$). (B) X-Y scatter plot visualizing the correlation between TBS and connD, as evaluated using DXA and μ -CT acquisitions, respectively. This high correlation is characterized by $R^2 = 0.67$ ($r = 0.82$, $p < 0.0001$). TBS, trabecular bone score; BMD, bone mineral density; DXA, dual-energy X-ray absorptiometry; connD, connectivity density; μ -CT, micro-computed tomography.

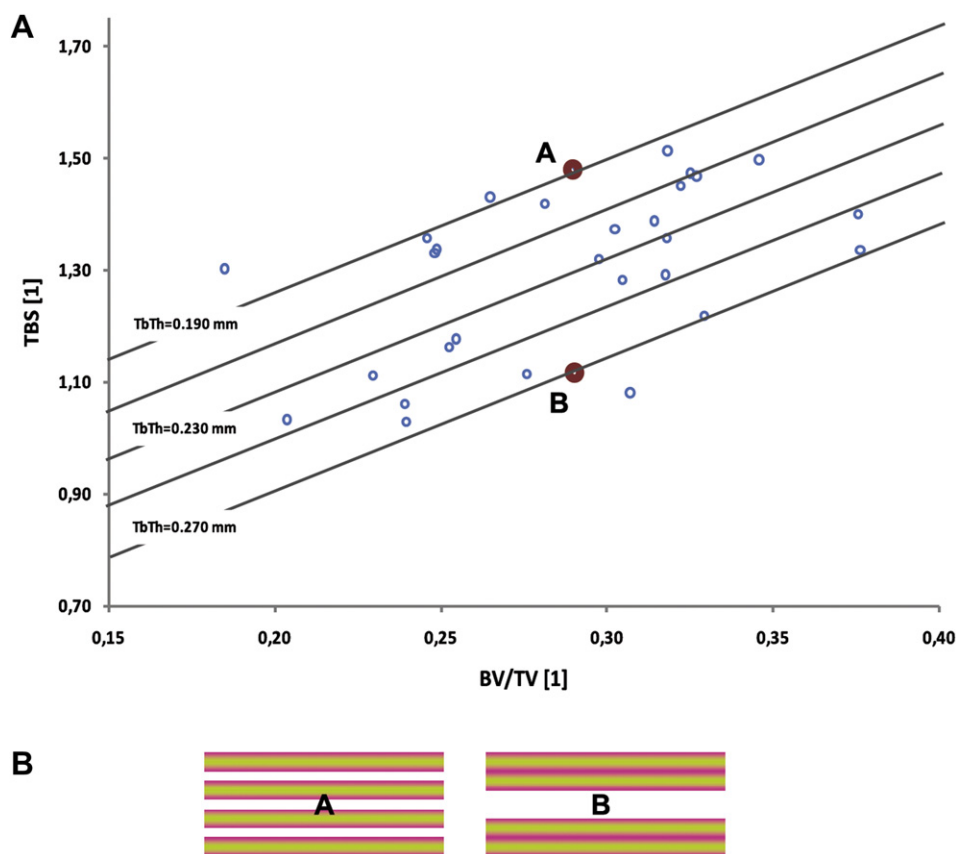


Fig. 4. (A) Two samples characterized by identical bone quantity (BV/TV) (and different trabecular thicknesses) are located on different isocurves, indicating significant differences in the TBS. (B) A model of representation with 2 patterns characterized by identical bone volume, exhibiting significant differences in bone microarchitecture, as expressed by TBS. BV/TV, bone volume/total volume; TBS, trabecular bone score; TbTH, trabecular thickness.

TBS ex-vivo reproducibility is good because the relative precision error and absolute precision error were 1.63% and 0.02, respectively. The TBS CV% precision value is consistent with those generally obtained for spine BMD CV% (40).

Hence, using multivariate linear regression modeling, we have established a model by which the relationship between TBS and 3D bone microarchitecture parameters could be interpreted, in particular BV/TV and TbTh. This model indicates that TBS adds more value and power of differentiation when samples with similar bone densities but different bone microarchitectures are studied (Fig. 5). In terms of diagnosing osteoporosis, it has been established (41) that about one-third of fragility fractures occur within DXA osteopenic or normal bone. This can be partially explained by the fact that BMD does not take into account alterations in bone microarchitecture; in other words, 2 individuals with similar bone mass may have different fracture risks because of the differences in their bone microarchitectures (Fig. 5B).

This ex vivo evaluation is quite similar to the ideal case (i.e., homogeneous soft tissue density, optimal AP vertebral positioning, no image inhomogeneity because of breathing, no bone marrow effect on the image). It seems to be clear

that, in in vivo conditions, the correlations between TBS and Parfitt's parameters should be impacted (i.e., decreasing correlation values in comparison with the ideal case) by soft tissue inhomogeneity, bone marrow, etc. However, clinical studies show that TBS has a high clinical add value. Applying TBS measurements to clinical DXA images, in combination or not with traditional BMD assessments, seems to be an effective and efficient way to improve our ability to diagnose osteoporosis and determine fracture risk.

This add value has been confirmed by several previously published clinical studies (28–35). More particularly, in an age- and BMD-matched case-control study (28), it was shown that TBS measured at the total spine (L2–L4) was significantly different between those with a fracture ($n = 45$) and those without ($n = 90$), when considering all types of fractures (odds ratio OR[95% Confidence intervals] = 1.95 [1.31–2.89], $p = 0.0005$) and vertebral fractures (OR = 2.66 [1.46–4.85], $p = 0.0004$). In another age-matched case-control study (30), focusing on osteopenic subjects with vertebral fractures, similar results were obtained after adjusting for weight with a TBS OR = 1.97 (1.31–2.96) and a BMD OR = 1.63 (1.20–2.22). More recently, in a retrospective analysis of a prospective study of 29,407 women (34),

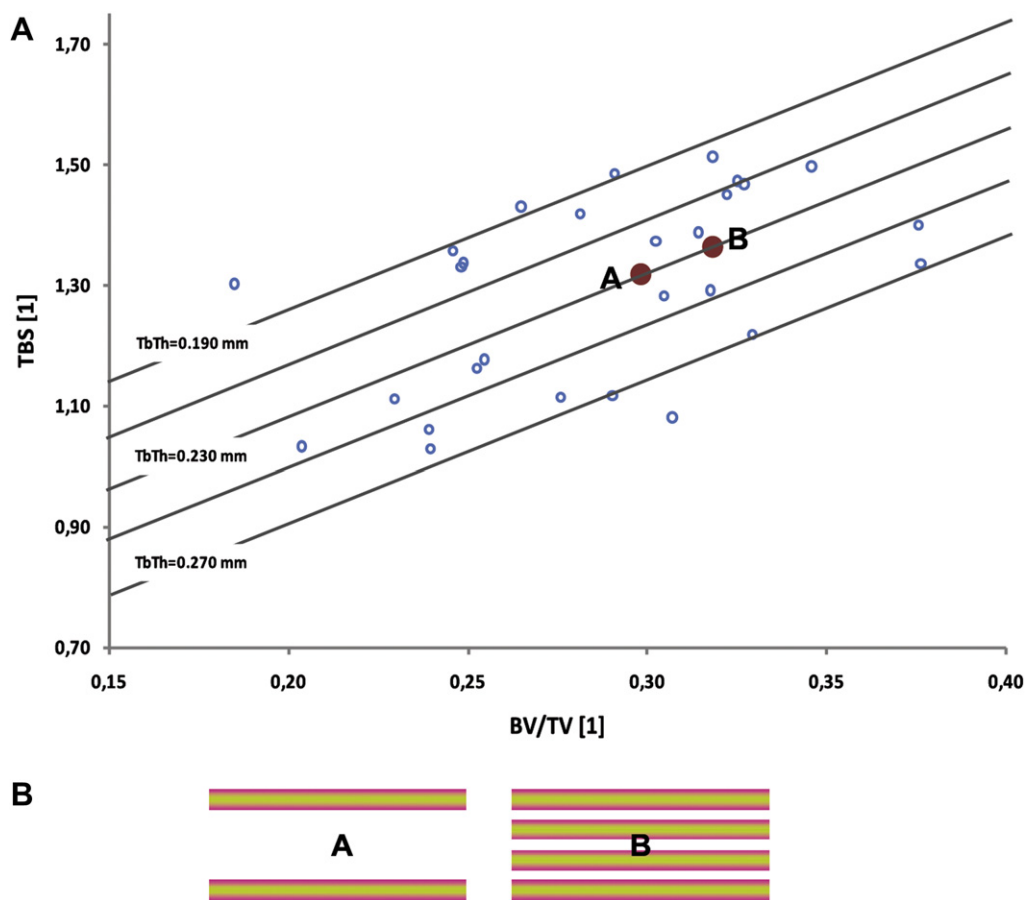


Fig. 5. (A) Two samples of identical TbTh are located on the same isocurve, indicating simultaneous variations in BV/TV and TBS but different amplitudes: relatively greater variation in BV/TV than TBS. (B) Model of representation with 2 patterns characterized by identical trabecular thickness and different bone volumes, indicating simultaneous variations in BV/TV and bone microarchitecture, as expressed by TBS. TbTH, trabecular thickness; BV/TV, bone volume/total volume; TBS, trabecular bone score.

it was shown that significantly lower spine BMD and spine TBS values were present in subjects with fractures than in those without fractures, when considering major OP fractures ($p < 0.0001$); the correlation between spine BMD and spine TBS was modest ($r = 0.33$); and BMD and TBS, evaluated at spinal levels L1–L4, predicted fractures equally well and independent of each other. In addition, TBS was found to be a relevant parameter in induced secondary osteoporosis (31–33).

In a retrospective study assessing the effect of glucocorticoids (GCs) on bone (31), GC-treated patients were characterized by a significant decrease in TBS ($p < 0.0001$) relative to age-matched normal values, whereas no change in BMD was observed ($p = 0.49$). Similar results were found even at 5 mg/d doses of GCs ($p = 0.0012$). GC-treated women experience a significant deterioration in bone microarchitecture, as assessed by TBS, which worsens with the presence, type, and number of fractures, and thus independently of BMD. Finally, in a retrospective study of 185 subjects suffering from rheumatoid arthritis (30 of 185 had at least 1 vertebral fracture), 8 of the 16 subjects with fractures, among the 128 subjects

with a T-score greater than -2.5 , were identified using TBS parameters (32).

Our present study has certain limitations. First, we used dried cadaveric vertebral specimens. This means that the effect of bone marrow on DXA acquisition and, consequently, on TBS was not taken into account. However, the presence of bone marrow should have a low impact on TBS. Using, for vertebra, the homogeneity of bone marrow distribution and composition hypothesis, it is clear that bone marrow presence had no effect on TBS, because TBS evaluation is based on pixel amplitude differences. In addition, to simulate abdominal soft tissue, we used a homogeneous soft tissue phantom that did not simulate DXA image inhomogeneity alterations created by the skin, muscles, fat, and viscera. The use of this phantom was motivated by the aim of this study not being to simulate real-life situations but to evaluate correlations between 3D microarchitecture parameters and DXA TBS values, minimizing confounding effects as much as possible. Finally, the potential effects of the projection type and posterior element projections were not evaluated in this study.

In conclusion, it has been shown that it is possible to estimate bone microarchitecture texture derived from DXA imaging using TBS. In this study, we demonstrated that gray-level variations in 2D-projection-based images, as evaluated by TBS, correlate well with certain characteristics of 3D microarchitecture: positively with connD and TbN, and negatively with trabecular spacing (TbSp) and solid volume fraction (BV/TV) in combination with TbTh. TBS seems to be a good surrogate non-invasive technique for assessing vertebral microarchitecture texture from DXA scans in routine clinical practice that would satisfy the definition of osteoporosis.

Acknowledgments

Sincere thanks to all personnel in the Anatomy Laboratory at the University Hospital of Bordeaux who assisted with the bone samples: Professors Dominique Midy and Jean-Marc Vital; Drs Benoît Lavignolle and Mathieu de Sèze; and Mr Jean-Jacques Barbouteau, Mr Etienne Delamarre, and Mr José Prata. Special thanks also to Aurelie Bergey for the DXA and μ -CT acquisitions. Finally, the authors want to thank Dr Alain Heraud, who granted them access to his Prodigy Device, and Kevin White from Science Right for English editing.

References

- Klibanski A, Adams-Campbell L, Bassford T, et al. 2000 Osteoporosis prevention, diagnosis, and therapy. NIH Consens Statement 17(1):1–36.
- Hordon LD, Raisi M, Aaron JE, et al. 2000 Trabecular architecture in women and men of similar bone mass with and without vertebral fracture: I. Two-dimensional histology. *Bone* 27: 271–276.
- Cummings SR, Nevitt MC, Browner WS, et al. 1995 Risk factors for hip fracture in white women. Study of Osteoporotic Fractures Research Group. *N Engl J Med* 332(12):767–773.
- Schuit SC, van der Klift M, Weel AE, et al. 2004 Fracture incidence and association with bone mineral density in elderly men and women: the Rotterdam Study. *Bone* 34:195–202.
- Wainwright SA, Marshall LM, Ensrud KE, et al. 2005 Hip fracture in women without osteoporosis. *J Clin Endocrinol Metab* 90:2787–2793.
- Rice JC, Cowin SC, Bowman JA. 1988 On the dependence of the elasticity and strength of cancellous bone on apparent density. *J Biomech* 21:155–168.
- Majumdar S. 1998 A review of magnetic resonance (MR) imaging of trabecular bone micro-architecture: contribution to the prediction of biomechanical properties and fracture prevalence. *Technol Health Care* 6:321–327.
- Turner CH, Cowin SC, Rho JY, et al. 1990 The fabric dependence of the orthotropic elastic constants of cancellous bone. *J Biomech* 23:549–561.
- Genant HK, Engelke K, Prevrhal S. 2008 Advanced CT bone imaging in osteoporosis. *Rheumatology* 47:9–16.
- Krug R, Carballido-Gamio J, Banerjee S, et al. 2008 In vivo ultra-high-field magnetic resonance imaging of trabecular bone microarchitecture at 7 T. *J Magn Reson Imaging* 27:854–859.
- Caligiuri P, Giger ML, Favus MJ, et al. 1993 Computerized radiographic analysis of osteoporosis: preliminary evaluation. *Radiology* 186:471–474.
- Samarabandu J, Acharya R, Hausmann E, et al. 1993 Analysis of bone X-rays using morphological fractals. *IEEE Trans Med Imaging* 12:e466–e470.
- Prouteau S, Ducher G, Nanyan P, et al. 2004 Fractal analysis of bone texture: a screening tool for stress fracture risk? *Eur J Clin Invest* 34:137–142.
- Gregory JS, Stewart A, Undrill PE, et al. 2004 Identification of hip fracture patients from radiographs using Fourier analysis of the trabecular structure: a cross-sectional study. *BMC Med Imaging* 4:4.
- Chappard D, Guggenbuhl P, Legrand E, et al. 2005 Texture analysis of X-ray radiographs is correlated with bone histomorphometry. *J Bone Miner Res* 23:24–29.
- Vokes TJ, Giger ML, Chinander MR, et al. 2006 Radiographic texture analysis of densitometer-generated calcaneus images differentiates postmenopausal women with and without fractures. *Osteoporos Int* 17:1472–1482.
- Bonnick SL. 2004 Bone densitometry in clinical practice application and interpretation. 2nd ed. Human Press Inc., Totowa, NJ.
- Genant HK, Wu CY, van Kuijk C, Nevitt MC. 1993 Vertebral fracture assessment using a semi-quantitative approach. *J Bone Miner Res* 8:1137–1148.
- Duboeuf F, Bauer DC, Chapurlat RD, et al. 2005 Assessment of vertebral fracture using densitometric morphometry. *J Clin Densitom* 8:362–368.
- Faulkner KG, Cummings SR, Black D, et al. 1993 Simple measurement of femoral geometry predicts hip fracture: the study of osteoporotic fractures. *J Bone Miner Res* 8:1211–1217.
- Center JR, Nguyen TV, Pocock NA. 1998 Femoral neck axis length, height loss and risk of hip fracture in males and females. *Osteoporos Int* 8:75–81.
- Beck TJ, Ruff CB, Warden KE, et al. 1990 Predicting femoral neck strength from bone mineral data. A structural approach. *Invest Radiol* 25(1):6–18.
- Nakamura T, Turner CH, Yoshikawa T, et al. 1994 Do variations in hip geometry explain differences in hip fracture risk between Japanese and white Americans? *J Bone Miner Res* 9(7): 1071–1076.
- Langton CM, Pisharody S, Keyak JH. 2009 Comparison of 3D finite element analysis derived stiffness and BMD to determine the failure load of the excised proximal femur. *Med Eng Phys* 31:668–672.
- Boehm HF, Vogel T, Panteleon A, et al. 2007 Differentiation between post-menopausal women with and without hip fractures: enhanced evaluation of clinical DXA by topological analysis of the mineral distribution in the scan images. *Osteoporos Int* 18:779–787.
- Piveteau T, Winzenrieth R, Hans D. 2011 Trabecular bone score (TBS) the new parameter of 2D texture analysis for the evaluation of 3D bone micro architecture status. *ECR*.
- Winzenrieth R, Piveteau T, Hans D. 2011 Assessment of correlations between 3D μ CT microarchitecture parameters and TBS: effects of resolution and correlation with TBS DXA measurements. *ECR*.
- Pothuau L, Barthe N, Krieg MA, et al. 2009 Evaluation of the potential use of trabecular bone score to complement bone mineral density in the diagnosis of osteoporosis: a preliminary spine BMD-matched, case-control study. *JCD* 12:170–176.
- Rabier B, Héraud H, Grand-Lenoir C, et al. 2010 A multicentre, retrospective case–control study assessing the role of trabecular bone score (TBS) in menopausal Caucasian women with low areal bone mineral density (BMDa): analysing the odds of vertebral fracture. *Bone* 46(1):176–181.
- Winzenrieth R, Dufour R, Pothuau L, et al. 2010 A retrospective case–control study assessing the role of trabecular bone

score in postmenopausal Caucasian women with osteopenia: analyzing the odds of vertebral fracture. *CTI* 86:104–109.

31. Colson F, Picard A, Rabier B, et al. 2009 Trabecular bone microarchitecture alteration in glucocorticoid treated women in clinical routine? a TBS evaluation. *JBMR* 24(S1):129.
32. Bréban S, Briot K, Kolta S, et al. 2010 Combination of bone mineral density and trabecular bone score for vertebral fracture prediction in secondary osteoporosis. *JBMR* 25(S1):53.
33. Maury E, Guignat L, Winzenrieth R, Cormier C. 2009 BMD and TBS micro architecture parameter assessment a spine in patients with anorexia nervosa. *JBMR* 24(S1):5.
34. Hans D, Goertzen AL, Krieg MA, Leslie W. 2009 Bone micro-architecture assessed by TBS at the AP spine predicts clinical spine fractures independently of BMD in 22234 women aged 50 and older: the Manitoba prospective study. *JBMR* 24(S1):38.
35. Boutroy S, Hans D, Vilaythiou N, et al. 2010 Trabecular bone score helps classifying women at risk of fracture: a prospective analysis within the OFELY Study. *JBMR* 25(S1):89.
36. Parfitt AM. 1983 The stereologic basis of bone histomorphometry. Theory of quantitative microscopy and reconstruction of the 3rd dimension. Recker R, ed. In *Bone histomorphometry technique and interpretation*. CRC Press, Boca Raton, FL, 53–87.
37. Parfitt AM, Drezner MK, Glorieux FG, et al. 1987 Bone histomorphometry: standardization of nomenclature. *J Bone Miner Res* 2:595–610.
38. Gluer CC. 1999 Monitoring skeletal changes by radiological techniques. *J Bone Miner Res* 14:1952–1962.
39. Dufour R, Heraud A. 2009 Lumbar spine microarchitecture in French women derived from DXA: TBS normative data. *JCD* 12(3):377.
40. Lewiecki E, Miller P. 2003 Precision comparison of two DXA densitometers—Prodigy and Delphi. *J Bone Miner Res* 18:205.
41. Miller PD, Barlas S, Brenneman SK, et al. 2004 An approach to identifying osteopenic women at increased short-term risk of fracture. *Arch Intern Med* 164:1113–1120.
42. Mandelbrot BB, Van Ness JW. 1968 Fractional Brownian motions, fractional noises and applications. *SIAM Rev* 10:422–437.

Appendix 1.

Trabecular Bone Score Concept Explanation

Trabecular bone score (TBS) development is based on the following facts:

- A healthy patient has well-structured trabecular bone at the vertebral level. This signifies that his trabecular structure is dense (i.e., high connectivity, high trabecular number, and small spaces between trabeculae). If we project this structure onto a plane, we obtain an image containing a large number of pixel value variations, but the amplitudes of these variations are small (**Fig. A1A**).
- Conversely, an osteoporotic patient has an altered trabecular bone structure. This signifies that his trabecular structure is porous (i.e., low connectivity, low trabecular number, and wide spaces between trabeculae). If we project this structure onto a plane, we obtain an image containing a low number of pixel value variations, but the amplitudes of these variations are high (**Fig. A1B**).

Consequently, if we can identify a method that differentiates these 2 types of structures, we can obtain a way to describe a 3-dimensional (3D) structure from the existing variations in its projected image. One way to achieve this is to calculate the variogram of the trabecular bone projected image, because it is calculated as the sum of the squared gray-level differences between pixels at a specific distance.

TBS is a black-box algorithm using the variogram after its log-log transformation. TBS is calculated as the slope of the log-log transformation of this variogram. This slope characterizes the rate of gray-level amplitude variations into the trabecular bone. Certain black-box differences render TBS not an H (Hurst parameter) estimator (42).

The following example (**Fig. A2**) illustrates how to evaluate a microstructure's quality from its macro-representation.

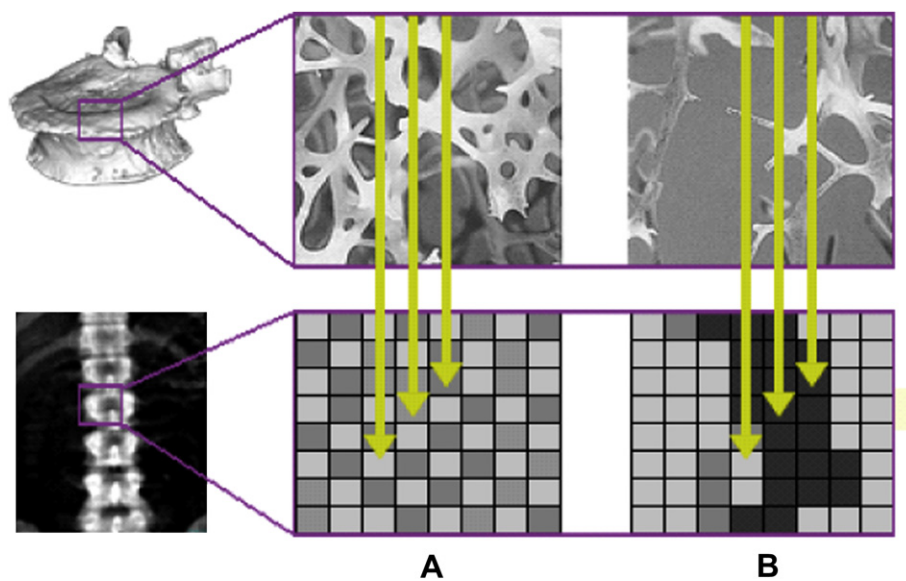


Fig. A1. Healthy (A) vs altered (B) trabecular structures.

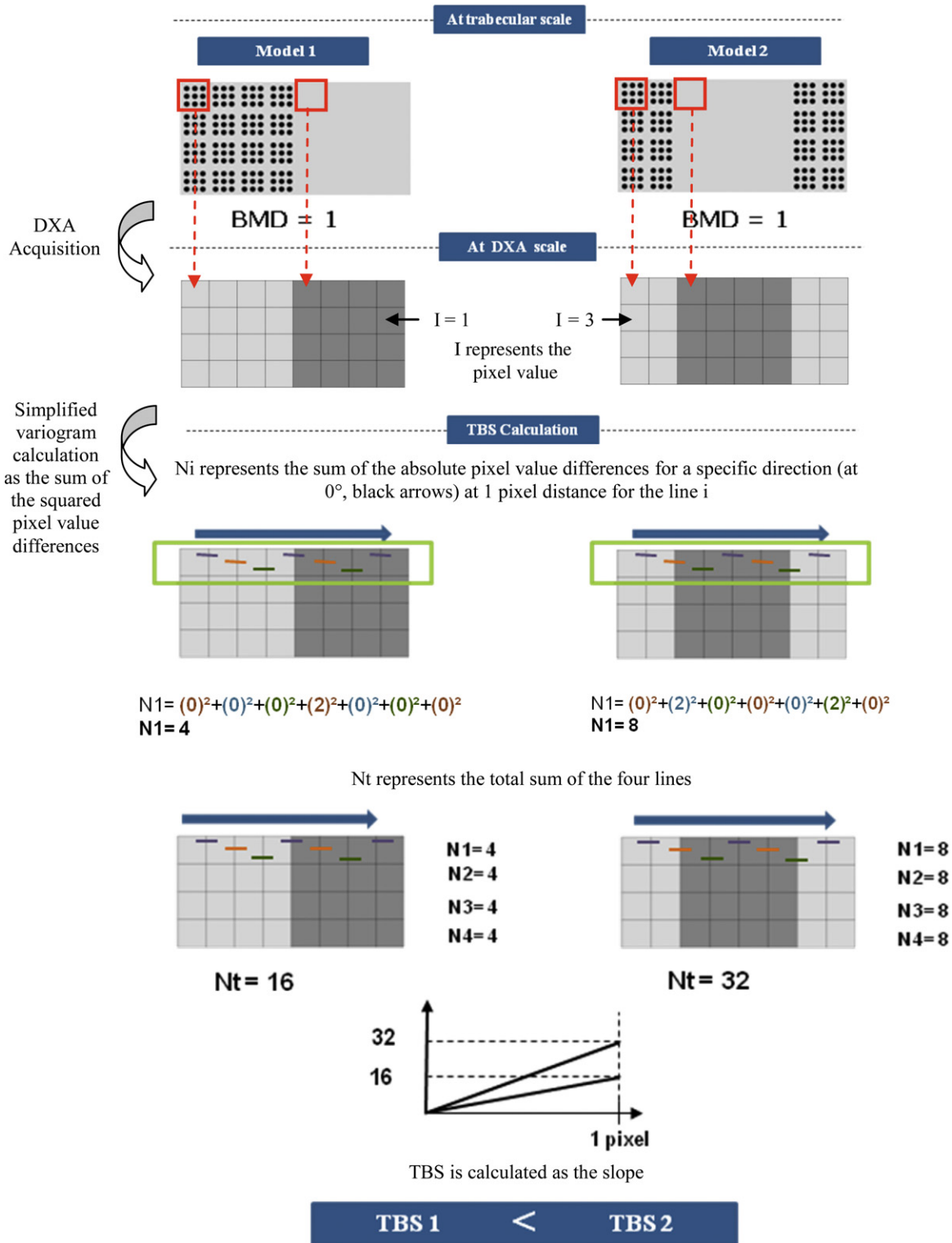


Fig. A2. TBS calculation example using 2 basic structures, composed of a plate and a set of rods. The 2 models of structure are composed of the same amount of bone. To simplify the TBS explanation, only 1 direction is taken into account, a distance of 1 pixel is used, and the final log-log transformation is omitted. TBS, trabecular bone score; BMD, bone mineral density; DXA, dual-energy X-ray absorptiometry.

This explanation is proposed for a basic structure and for a simplified process (only considering an exploration distance of 1 pixel, without the final log-log transformation) to present the methodology clearly.

From this example, it is easy to understand that resolution will have an impact on pixel size, but not on pixel variations, which are related to microstructure status. However, the number of pixels in the region of interest investigated must be sufficient to generate a good estimate of the microstructure (small standard error of the estimate).

Appendix 2.

Model of Interpretation for Trabecular Bone Score

Step 1—Trabecular Bone Score, a Model of Connectivity

TBS was significantly correlated with connectivity density (connD) through the following generic linear regression equation:

$$\text{TBS} = F_1(\text{connD}) = a_1 + b_1 * \text{connD} \quad (1)$$

To optimize the evaluation of (a_1, b_1) fit coefficients, several sample subsets were considered, including 10 subsets of 20 samples and 10 subsets of 10 samples. Each of these subsets was randomly generated from the global set of 30 samples.

A couple of fit coefficients (a_1, b_1) were determined by linear regression analysis for each of the 20 sample subsets, leading to the following mean fit coefficients: $a_1 = 0.893$ and $b_1 = 0.086$. The precision of this mean model was evaluated as the mean precision of the model of each subset, expressed by an RMS error of 0.041:

$$\begin{aligned} F_1(\text{connD}) &= 0.893 + 0.086 * \text{connD} \\ \text{TBS} &= F_1(\text{connD}) \pm 0.041 \end{aligned} \quad (2)$$

Step 2—Connectivity, a Multivariate Model

ConnD is a topology-based 3D parameter of bone microarchitecture, which is not easy to interpret. To facilitate this interpretation, we have expressed connD as a function of the bone volume/total volume (BV/TV) and trabecular thickness (TbTh) parameters:

$$\begin{aligned} \text{connD} &= F_2(\text{BV/TV}, \text{TbTh}) \\ &= a_2 + b_2 * \text{BV/TV} + c_2 * \text{TbTh} \end{aligned} \quad (3)$$

This linear multivariate regression model was highly predictive ($R^2 = 0.95$) and statistically significant, with the p value for both cofactors lower than 0.0001.

Step 3—Trabecular Bone Score, a Multivariate Model

Combining Eqs. (1) and (3), TBS was determined as a multivariate linear regression model incorporating both BV/TV and TbTh:

$$\begin{aligned} \text{TBS} &= F(\text{BV/TV}, \text{TbTh}) = \alpha + \beta * \text{BV/TV} + \delta * \text{TbTh} \\ \alpha &= a_1 + (b_1 * a_2) \\ \beta &= b_1 * b_2 \\ \delta &= b_1 * c_2 \end{aligned} \quad (4)$$

The fit coefficients $(\alpha, \beta, \text{ and } \delta)$ were determined, taking into account both Eqs. (1) and (3), for each of the 20 sample subsets, leading to the following mean fit coefficients: $\alpha = 1.630$, $\beta = 2.379$, and $\delta = -4.456$. The precision of the mean model was evaluated as the mean precision of the model of each subset, expressed by an RMS error of 0.043:

$$\begin{aligned} F(\text{BV/TV}, \text{TbTh}) &= 1.630 + 2.379 * \text{BV/TV} - 4.456 * \text{TbTh} \\ \text{TBS} &= F(\text{BV/TV}, \text{TbTh}) \pm 0.043 \end{aligned} \quad (5)$$